# From magnetic cluster glass state to giant vertical magnetization shift induced by ferromagnetic cluster growth in SrFe0.25Co0.75O2.63

Madhu Chennabasappa, Alain Pautrat, Olivier Toulemonde

# From magnetic cluster glass state to giant vertical magnetization shift induced by ferromagnetic cluster growth in $SrFe_{0.25}Co_{0.75}O_{2.63}$

**Madhu Chennabasappa [a, b], Alain Pautrat [c], Olivier Toulemonde [a, *]**

*[a] CNRS, Université de Bordeaux, ICMCB, UPR 9048, F-33600 Pessac, France.*

*[b] Department of Physics, Siddaganga Institute of Technology, BH Road, Tumakur – 572103, India.*

*[c] CRISMAT, CNRS, Normandie Univ, ENSICAEN, UNICAEN, 14000 Caen, France*

**olivier.toulemonde@icmcb.cnrs.fr*

Abstract: A charge ordering phenomenon within the crystallographic sites as following $Sr_4(Fe_{0.14}^{3+}Co_{0.36}^{3+})_4^{8h}(Fe_{0.11}^{4+}Co_{0.14}^{4+}Co_{0.25}^{3+})_4^{8f}O_{10.52}$ was previously reported thanks to neutron diffraction coupled with Mossbauer spectroscopy studies. Such distribution supports a natural magnetic layered structure combining both in-plane ferromagnetic super-exchange interactions mainly on the octahedron "8f" sub-layer alternating and in-plane antiferromagnetic super-exchange interactions on the "8h" sub-layer containing tetrahedral sites and five-fold symmetry polyhedra (i.e. squared based pyramid and/or trigonal bipyramid). Because of the interfacial magnetic interactions between the two types of layers, we report a detailed study of the intriguing magnetic properties. AC magnetic susceptibility shows a frequency dependent peak suggesting a cooperative character due to inter-cluster interactions resulting in a magnetic cluster glass state. When temperature decreases and/or applied magnetic field increase, the ferromagnetic clusters growth is promoted and results in a large vertical hysteretic shift on the Field Cooled magnetization isotherm in relation with minor loop.

The occurrence of horizontal and/or vertical hysteretic shift of the magnetic loop [1] attracted attention in solid-state physics and materials chemistry communities. Leading to horizontal shift of the magnetic hysteresis loop, the so-called exchange bias (EB) is ascribed to interactions between ferromagnetic (FM) and antiferromagnetic (AFM) layers. Positive or negative exchange bias occurs when a positive or negative horizontal hysteretic shift is seen depending on the sign of the cooling field. Historically, EB effect was evidenced by Meiklejohn and Bean [2] in nanostructured Co/CoO system with Co as ferromagnetic (FM) phase and CoO as antiferromagnetic (AFM) phase before being extended to binary alloys [3] - Nogués and Schuller review the phenomenology of exchange bias and related effects [4]. Interestingly, it is more recently that vertical hysteretic shift was pointed out either in artificial bilayered material [5] or in natural materials. In the latter case, the vertical hysteretic shift is often structurally related to either oxygen vacancies as seen in layered ferrite $Sr_4Fe_4O_{11}$ [6] or cobaltite $Sr_3YCo_4O_{10.5}$ [7] or in the intrinsic layered Ruddlesden-Popper (*RP*) $Sr_{1.5}Pr_{0.5}CoO_4$ [8] phases. However, some controversies about its origin were pointed out [9] due to the large number of factors like interfacial interactions between different magnetic phases, macroscopic separated phases and/or magnetic training effect.

Few years ago, an exchange bias and memory effect was reported in the perovskite $SrFe_{0.5}Co_{0.5}O_{3-\delta}$ [10]. The given crystalline framework $Sr_2FeCoO_6$ based on “rock-salt”-type ordering [11] is likely not valid because the stabilisation of such very high $Fe^{4+}$ and $Co^{4+}$ oxidation states require drastic synthesis conditions [12]. Indeed $SrFe_{0.5}Co_{0.5}O_3$ is simple cubic perovskite with ferromagnetic transition close to room temperature [13]. However, the reported magnetic properties are likely intrinsic. Furthermore, an oxygen vacancies ordering model in $SrFe_{1-x}Co_xO_{3-\delta}$ oxygen deficient mixed iron/cobalt perovskite has been reported [14]. And, when Fe/Co ratio is changed, the coexistence of nearly compensated and ferrimagnetic regions in the oxygen vacancies layered structure leads to magnetoresistance and more likely vertical shift than exchange bias [15].

Previously, detailed investigations of $SrFe_{0.25}Co_{0.75}O_{2.63}$ material by means of Mössbauer spectroscopy, Mohr salt titration and neutron diffraction using the Fe and Co neutron cross sections contrast, have been carried out. Such an approach allows us to propose a crystallographic formula as the following $Sr_4(Fe_{0.14}^{3+}Co_{0.36}^{3+})_4^{8h}(Fe_{0.11}^{4+}Co_{0.14}^{4+}Co_{0.25}^{3+})_4^{8f}O_{10.52}$ [16] . It supports a natural layered structure with high Fe and Co oxidation states in the oxygen

replete layers. Following the structural and chemical investigations of our $SrFe_{0.25}Co_{0.75}O_{2.63}$ material, the magnetic properties were carried out using commercial MPMS SQUID (Quantum Design, USA) instrument. Our results suggest that our natural framework shows similarly behavior than the one observed in ferromagnetic / antiferromagnetic heterostructure resulting in a biased coercive field leading to giant vertical shift magnetization. Its magnitude can then be tuned either by the temperature or by the applied magnetic field.

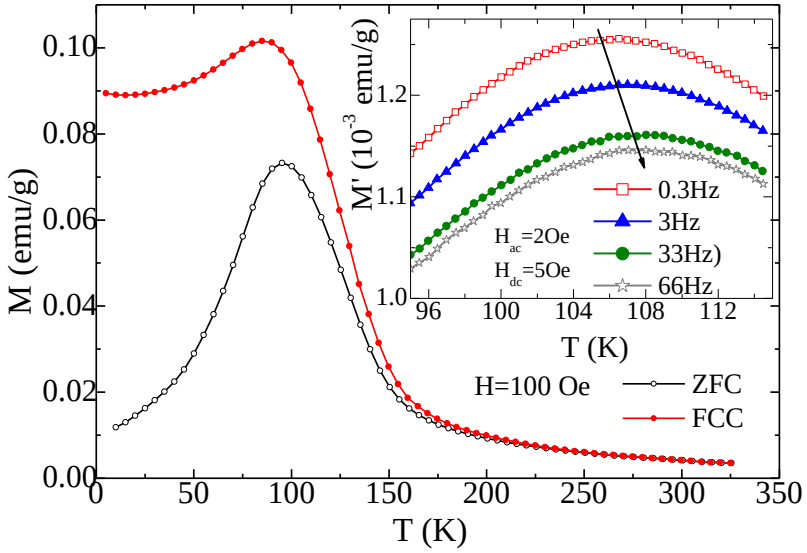


**Figure 1:**

Typical Zero Field Cooled (ZFC) and Field Cooled Cooling (FCC) magnetization curves

Inset displays Real part of the AC susceptibility at different frequency

As shown in figure 1, magnetization measurements under 0.01T on $SrFe_{0.25}Co_{0.75}O_{2.63}$ material reveal a weak magnetic peak around 95 ± 5K. Further, a deviation between data collected in a field-cooled mode (FCC) and a zero field cooled mode (ZFC) is observed. It becomes larger and larger when cooling with a clear asymptotic divergence around 150K whereas the Curie-Weiss law divergence already occurs around 310K (see Supplementary material S1 & S2 figures). Such a thermal hysteretic behaviour and the magnetic peak temperature were expected in view of similar measurements carried out on layered $SrFeO_{3-\delta}$ [17] and $SrFe_{0.5}Co_{0.5}O_{3-\delta}$ [11]. Below 50K, similar constant branch on the FCC curve has already been observed either in ferromagnetic clusters embedded in a weakly magnetic matrix in a concentrated nanoparticles system [18]. But it has also been observed in cation ordered perovskite being the signature of long-range magnetic frustration due to competing nearest and next nearest neighbor superexchange interaction [ 19 ]. AC magnetization measurements at different frequency were then carried out to better characterize that behavior. Peak position on the real part of the AC magnetization around the main peak shows a frequency dependent shift (see inset of figure 1) that rules out the possibility of any long-range magnetic

ordering at the peak temperature defined as $T_f$ for freezing temperature. To better understand the nature of the frequency dependence of $T_f$, our data has been analyzed using the empirical Vogel-Fulcher (VF) law expected for magnetically interacting clusters [20] because a Néel-Arrhenius law expected for superparamagnetic systems [ 21 ] results in very unphysical parameters as illustrated in the supplementary material (figure S3). The empirical Vogel-Fulcher law given by

$$\tau = \tau^* \exp\left(\frac{E_a}{k_B(T_f - T_0)}\right),$$

with three fitting parameters i.e. $\tau^*$ the characteristic attempt time, $E_a$ the average thermal activation energy and the Vogel-Fulcher $T_0$ having value between 0 and $T_f$ that is often interpreted as a measure of inter-cluster interaction strength, The frequency dependence of the freezing temperature $T_f$ using the VF approach shown figure 2a gives reasonable parameters.

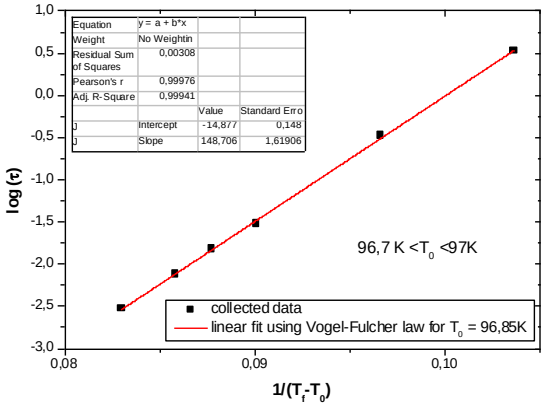


**Figure 2a :**

The frequency dependence of freezing temperature plotted as a log($\tau$) vs $1/(T_f - T_0)$.

Fit parameters obtained from the Vogel-Fulcher law are sum up in table1.

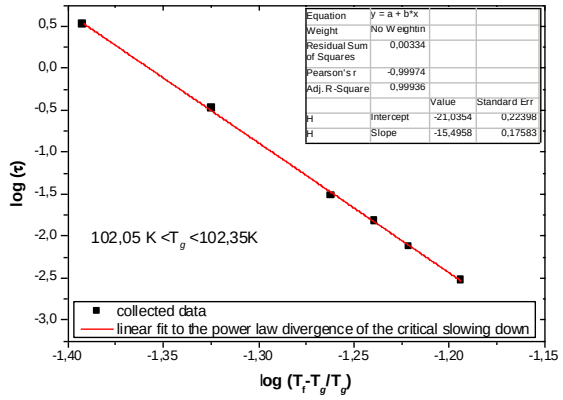


**Figure 2b :**

The frequency dependence of freezing temperature plotted as a log($\tau$) vs $\log(T_f - T_G)/T_G)$.

Fit parameters obtained from the power law divergence are sum up in table 1.

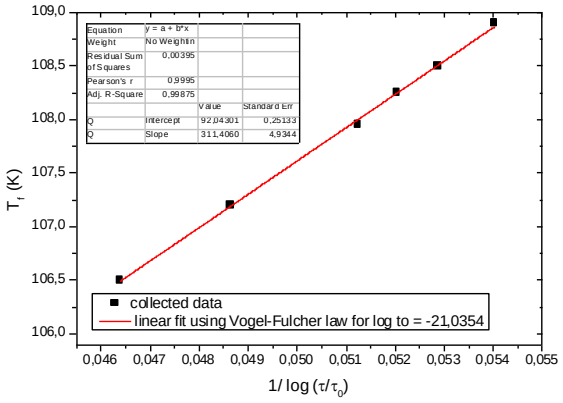


**Figure 2c :**

The frequency dependence of freezing temperature for a fixed characteristic attempt time to 5.08 $10^{-10}$s plotted as $T_f$ vs $1/\log(\tau/\tau_0)$.

Fit parameters obtained from the Vogel-Fulcher law are sum up in table1.

The $T_0$ value ranges between 96.7 K < $T_0$ < 97.0 K was first estimated minimizing the fitting error for a fixed $T_0$ value. Interestingly, $T_0$ nicely matches with the ZFC peak obtained under 100 Oe in the DC magnetic susceptibility. Then $E_a/k_B$ and $\tau^*$ were obtained from the slope and the intercept of $\log\tau$ versus $1/(T_f-T_0)$ fixing $T_0$ value at 96.85K. It results in parameters ranging between 142.5 K < $E_a/k_B$ < 155.0 K and 2.45 $10^{-7}$s < $\tau^*$ < 4.8 $10^{-7}$s respectively. First, $E_a/k_B$ temperature range well matches with the one at which an upturn is seen in the difference between ZFC and FCC magnetic DC susceptibility as seen in supplementary material figure S1. Surprisingly, it also matches with the one obtained using the same empirical law for rich iron perovkite $SrFe_{0.90}Co_{0.10}O_{3-\delta}$ [22] for which Co/Fe ratio is reversed with respect to our sample. The average strength of the super exchange magnetic interactions involved in $SrFe_{0.90}Co_{0.10}O_{3-\delta}$ and our $SrFe_{0.25}Co_{0.75}O_{2.63}$ compounds seems on the same range. Secondly, $\tau^*$ range value is typical for spin cluster glass ($10^{-9}$–$10^{-6}$ s) supporting a cooperative character due to inter-cluster interactions and not a single atomic spin dynamic ($10^{-13}$s). This is further supported by the Tholence's criterion [23] $T^* = (T_f-T_0)/T_0$ ranging from 0.09 to 0.11 and by the ratio $Ea/k_BT_f$ ranging from 1.30 to 1.45. Both Vogel Fulcher parameters amplitudes are comparable to those of frustrated spin glass on a concentrated system with ferromagnetic and antiferromagnetic interactions [24] or for short-range interactions magnetic glass as observed in $Eu_{0.5}Gd_{0.5}S$ material [23]. Then, to quantify the spin glass transition temperature, the frequency dependence of $T_f$ has been studied by the dynamic scaling theory [25] (see figure 2b)

$$\tau = \tau_0 \left(T_f/T_g - 1\right)^{-z\nu},$$

where $\tau$ is the dynamical fluctuation time scale corresponding to measurement frequency at the peak temperature, $\tau_0$ is here the microscopic flipping time for fluctuating entities, $T_g$ is the spin cluster glass transition temperature in the limit of zero frequency, and z and $\upsilon$ are the critical exponents. First, the best scaling relation is obtained for the following set of parameters with

102.05K < $T_g$ < 102.35 K, 15.3 < zυ < 16.6 and 2.8 $10^{-10}$s < $\tau_0$ < 9.3010$^{-10}$s. The value of exponent zυ is higher to that observed in case of Fe doped cobaltites perovskite structure [11,26] but in the order of magnitude of others mixed cobaltite insulating oxides [27] in which a large distribution of ferromagnetic and antiferromagnetic super exchange interactions is reported. Finally, the characteristic attempt time $\tau^*$ for the empirical Vogel-Fulcher law was fixed to the value of the microscopic flipping time for fluctuating entities to 5.08 $10^{-10}$s obtained at $T_g$ = 102.2K. The parameters 91.8 K < $T_0$ < 92.3 K and 306 K < $E_a/k_B$ < 316 K (see figure 2c) can then be extracted thanks to the empirical Vogel-Fulcher law from the intercept and the slope respectively. It appears that $T_0$ parameter is not really impacted by characteristic attempt time adjustment contrary to $E_a/k_B$. The $E_a/k_B$ temperature range is now unambiguously matching with the temperature at which the paramagnetic Curie-Weiss law is lost and with the ferrimagnetic ordering temperature of a similar compounds $SrFe_{0.15}Co_{0.85}O_{2.62}$ [14]. Furthermore the ratio $Ea/k_BT_f$ ranging from 2.81 to 2.97 always nicely matches that obtained for $Eu_{0.5-x}Gd_{0.5+x}S$ materials characterized as frustrated spin glass [23].

As an intermediate conclusion, from a dynamic scaling theory analysis, the low temperature magnetic behavior of our $SrFe_{0.25}Co_{0.75}O_{2.63}$ material is significant of magnetic clusters stabilization that are frozen at "macroscopic" time scales below $T_g$ = 102.20 ± 0.15 K and fluctuate above it. Clusters growth occurs at different scale of temperature, likely depends on the local oxidation state distribution in the layered structure, and then, on the distribution of magnetic super-exchange interactions. Two preferential growth temperatures are then suggested. A first one's occurring around 310 K in relation with the Vogel-Fulcher $T_0$ = 92.05 ± 0.25 K and the characteristic attempt time $\tau^*$ = 5.08 $10^{-10}$s as supported by the thermal activation temperature ranging 306 K < $E_a/k_B$ < 316 K related to the loss of the Curie –Weiss behavior for the DC magnetic susceptibility data. A second one's would occur around 150K in relation with the Vogel-Fulcher $T_0$ = 96.85 ± 0.15 K and the characteristic attempt time $\tau^{*'}$ = 3.45 $10^{-7}$s as supported by the average thermal activation temperature range between 142.5 K < $E_a/k_B$ < 155.0 K which matches with the asymptotic temperature behavior of the DC susceptibility difference between the ZFC and FCC process. That is why, regarding (i) the layered character of our $SrFe_{0.25}Co_{0.75}O_{2.63}$ material, (ii) its frozen spin cluster glass state below 102.2 K and (iii) the long-range magnetic ordering observed around room temperature in related $SrFe_{0.15}Co_{0.85}O_{2.62}$ oxide [14], the possibility of any vertical and/or horizontal hysteretic shift phenomenon has been probed.

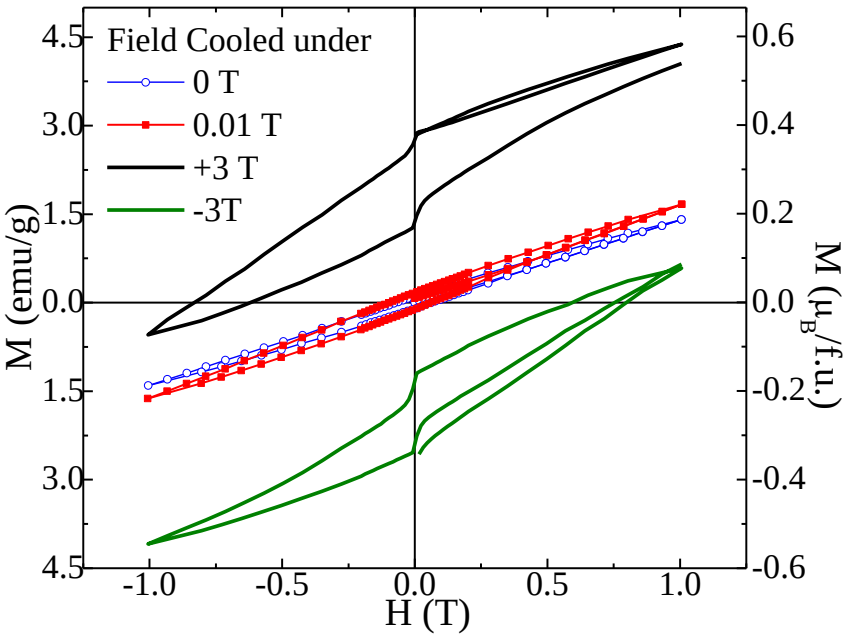


**Figure 3:** Isothermal magnetization curves at 15K after ZFC or FCC under different applied field.

Figure 3 shows four isothermal magnetization curves versus applied magnetic field carried out at 15K. Already a small deviation of the hysteresis loop is highlighted after cooling the sample from RT under 0.01T regarding the standard measured after a ZFC process. Both a squared broadening of the hysteresis curve and a slight vertical shift of the magnetization i.e., in the direction of the applied field are observed and unambiguously improved when applied field amplitude increases suggesting the combination of ferromagnetism and spin cluster glass state [28]. Furthermore, an application of +3T shifts the magnetization towards positive axis while reversing the field to -3T results in a shift towards negative magnetization. The amplitude of the phenomenon in our material is not of the same order of magnitude as those published till date. Indeed, almost the entire loop changes its sign. Let us recall that a giant vertical hysteretic shift of 35% at 2 K under ±7T was considered in $La_{0.3}Sr_{0.7}FeO_3$ (110nm)/SrRuO3 (10nm) bilayer on STO substrate [5] while our effect is in the order of magnitude of 85% at 15K under ±3 T. To characterize such a high asymmetry, isothermal magnetization loop starting from 14T was made in purpose as previously pointed by Geshev [29] (see supplementary material S4 figure). The magnetization saturation that is never reached under such experimental limit, could roughly be estimated around $2.5\mu_B/Sr_4FeCo_4O_{10.5}$. This relatively low magnetic saturation is typical of a magnetic frustrated system. The frustration occurs at a long-range scale due to competing nearest and next nearest neighbor superexchange interactions. And, the vertical hysteretic behavior of magnetization when the material is cooled under ±3 T is thus likely due to minor loop in relation with ferromagnetic clusters aligned by an external magnetic field. It is not a conventional exchange bias phenomenon [28].

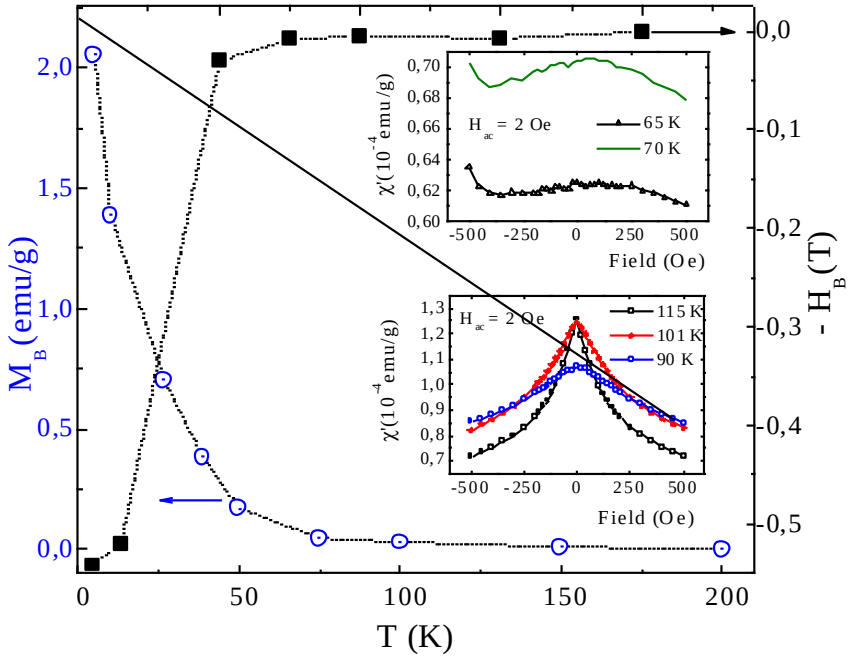


**Figure 4:** Temperature dependence of - $H_{Bias}$ (square) and $M_{Bias}$ (circle) extracted from the isothermals shown figure S8. *The dot lines are guides to the eyes*.

Insets show low field variation of AC χ' (33Hz) magnetization for selected temperatures.

The magnitude of the magnetic interactions involved in that biased phenomenon were quantitatively estimated. Series of loops were collected at different temperatures after cooling the sample from room temperature under 3T. At each temperature, parameters $H_{Bias}$ and $M_{Bias}$ were extracted according to $H_{Bias}= - (H_L+H_R)/2$ where $H_L$ and $H_R$ are the left and right field at which the magnetization is zero and $M_{Bias} = (M_1+M_2)/2$ where $M_1$ and $M_2$ are the magnetization values at H = ±1T respectively. Most of the collected isothermal magnetization curves are proposed in the supplementary material S5 figure and all the data treatment results are displayed in figure 4. For temperatures above 50K, $M_{Bias}$ and $H_{Bias}$ amplitudes are about constant becoming nearly zero at higher temperature. However, as temperature decreases below 50K, there is a clear enhancement of both $M_{Bias}$ and $H_{Bias}$ in relation with the occurrence of a squared-like loop. This temperature around 50K is quite low in comparison with the spin cluster glass transition temperature $T_g$ but better coincides with the slight upturn seen in the DC FCC magnetic susceptibility (Figure 1) and with the spin cluster glass transition state proposed in $Sr_4Fe_4O_{11}$ perovskite [30]. The real part isothermal AC magnetization curves under low applied field were then carried out. As shown in the lower insets of figure 4, the magnetic field dependence is first kept symmetric through the paramagnetic state (115K) to the spin cluster glass state (90K) transition while a clear breaking of the symmetric response implying the existence of a spontaneous magnetic moment as seen at lower temperature (65K (black circle with line) and 70K (green line) - upper inset of figure 4) [31]. Such a breaking of the symmetric

response is even enhanced when temperature is further decreased. It unambiguously supports long range magnetic ordering at the used frequency probe.

In addition, from isothermal minor loop magnetization curves collected at 15K after cooling the sample from RT under different magnetic excitation, both the squared loop size and the vertical shift increase with applied magnetic field as seen figure S6. All our magnetization measurements definitively suggest the stabilization of ferromagnetic clusters whose (i) magnetization directions are aligned along the applied field direction when cooling and (ii) sizes are promoted either by the increase of the applied field amplitude when cooling or by lowering the temperature below 50K.

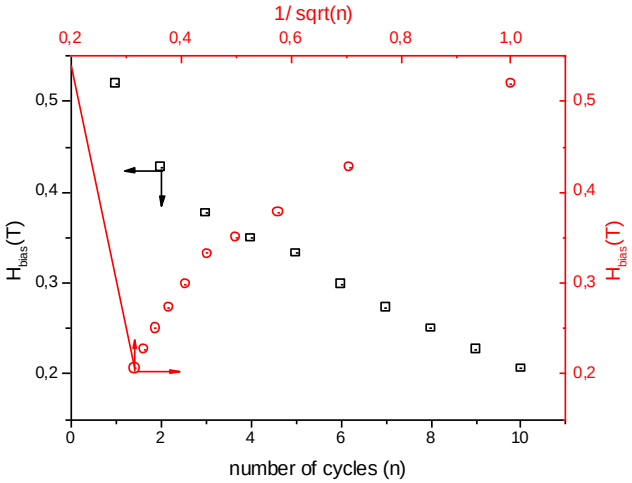


**Figure 5 :** Decrease of the bias field ($H_{bias}$) with the consecutive number (n) of cycles of the hysteresis loop (bottom & left axis) or with 1/sqrt(n) (top & right axis) exhibiting a so-called training effect.

The training effect is an important characteristic related to the gradual decrease of the anisotropy interaction commonly found on the exchange bias systems and interpreted by a spin configurational relaxation mode [32]. It is described by a quantitative power law along n consecutive cycles [33] $H_{bias}(n) - H_{E\infty} = \kappa/\mathrm{sqrt}(n)$ where $\kappa$ is both system and experiment dependent constant and $H_{E\infty}$ is the bias field in the limit of infinite loops and has been measured at 15K for the present sample after cooling the sample from RT under 3T. Up to 10 consecutive minor MH loops have been collected and plotted in figure Supplementary material S7. Figure 5 is focused in the dependence of bias field ($H_{bias}$) as defined previously along the 10 consecutive cycles. The quantitative power law is satisfied giving in a $H_{bias}$ contraction. Interestingly, two different regimes are indeed depicted. Considering the last cycles, $|H_{E\infty}| = 0.091 \pm 0.013$ T is expected from the intercept of the linear fit (see supplementary material S8 figure). That is why, as already reported in $Mg_{0.5}Mn_{2.5}O_4$ [34] spinel oxide the question is how much our loop displacements are associated with the magnetic viscosity defined as

S = dM/dln(t) where M is the magnetization and t the elapsed time. The magnetization (see figure 6a) and the bias field (see figure 6b) time dependence along the consecutive number of cycles collected at 15K were then plotted in a time log scale.

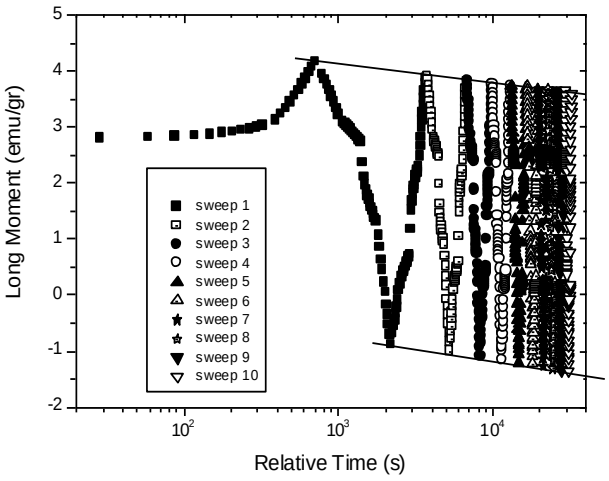


**Figure 6 a.**

The magnetization time dependence in a log scale along the consecutive number of cycles of the hysteresis loop collected at 15K. The up (down) branches are due to the applied field in(de)creases. The solid lines are linear fit for a fixed temperature (15K) and applied magnetic field (+1T in top and -1T in the bottom).

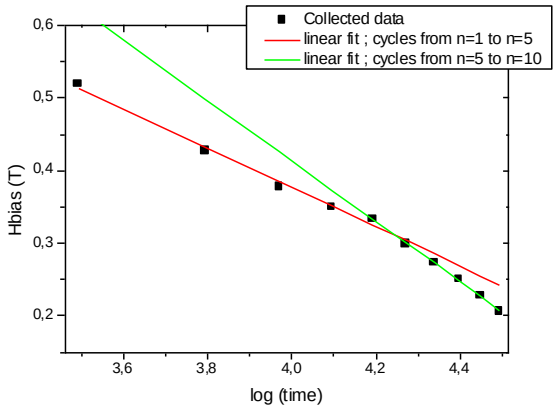


**Figure 6 b.**

Decrease of the bias field ($|H_{bias}|$) with the time of the hysteresis loop collected at 15K. Each cycle is about 3117s in average. The solid lines are linear fits.

The magnetization relaxation phenomenon is here investigated as follows, the magnetization as function of time under a given applied magnetic field lower than the applied during the cooling process. Two extremes M(±1T, 15K, t) linear behavior are underlined figure 6a and they obeyed to the magnetic viscosity's log scale time law resulting in $5.4\ 10^{-3} < S(1T,15K) < 5.8\ 10^{-3}$ (a.u) and $7.3\ 10^{-3} < S(-1T,15K) < 7.9\ 10^{-3}$ (a.u). The observed logarithmic dependence of the magnetization in spin glass systems means that the relaxation of the system is determined by a broad distribution of activation energies. This is indeed expected for our materials exhibiting a large distribution in magnetic exchange constant sign and/or amplitude considering all the nearest and the next nearest magnetic interactions plus the chemical distribution. Then the two previously reported regimes for the bias field are also underlined in figure 6b showing

two different logarithmic dependence of the bias field. A slightly modified magnetic viscosity law with the equation $H_{bias}$ *(*or *M(±1T, 15K, t)) = const + S1n(t/τo),* where *t* is the elapsed time since changing the field and *τo* the characteristic time of the relaxation has been checked. However unsuccessful tests were carried out aiming to extract from our data any characteristic time of the relaxation arising either from the thermal fluctuation of the bias field or from the magnetization. Even if a *τo* of 100s was inputted as observed in the case of phase separation manganites perovskites [35], a large range of fixed *τo* from 100s to $10^{-10}$s can been imputed giving similar linear quality factors. Consequently, it is tempting to speculate consecutive loop displacements with the magnetic viscosity moving the state of the sample toward an ideal not displaced loop as the apparent equilibrium at much larger time scale.

The ferromagnetic clusters are originated from the ferromagnetic $Fe^{4+}$-O(2p)-$Co^{4+}$, $Co^{4+}$-O(2p)-$Co^{4+}$ and $Co^{3+}$-O(2p)-$Co^{4+}$ superexchange interactions. Their interaction strengths are large enough to induce ferromagnetic ordering around room temperature in $Sr_{1-x}La_xCoO_3$ ($0<x<0.5$) [36] and $SrFe_{1-x}Co_xO_3$ ($0.2<x<1$) [37]. Interestingly, we already pointed out the following iron and cobalt distribution in the crystalline framework with $Sr_4(Fe_{0.56}{}^{3+}Co_{1.44}{}^{3+})^{8h}(Fe_{0.44}{}^{4+}Co_{0.54}{}^{4+}Co_{1.02}{}^{3+})^{8f}O_{10.52}$. One can then expect that ferromagnetic cluster grow around room temperature resulting from preferential in-plane ferromagnetic super-exchange interactions on the octahedron "8f" sub-layer. The slight deviation observed in the inverse magnetic susceptibility around room temperature likely result from those clusters behaving independently from each other's. When the temperature decreases, the nearest antiferromagnetic super exchange interactions as for example $Fe^{3+}$-O(2p)-$Co^{3+}$ and $Fe^{3+}$-O(2p)-$Fe^{4+}$ start to be active [6] that would pin clusters becomes significant. It results in the upturn around 150K seen in the difference between the DC magnetic susceptibility curves collected in a ZFC and FCC process under 100 Oe. With further temperature decreases, as supported by the frequency dependence of our AC susceptibility, a magnetic phase transition toward a spin cluster glass state takes place around 95 K. The broad distribution in sign and amplitude of the exchange coupling factors is at the origin of the broad size clusters. The spin cluster glass state resulting from the freezing of the different size clusters. Such magnetic frustration at the clusters interface precludes any long range magnetic ordering [14].

Interestingly, if one considers the previous study for $SrFe_{0.15}Co_{0.85}O_{2.62}$ [15], magnetic moments at the 8h crystallographic site i.e. in the oxygen deficient layers is in average higher than those at the 8f crystallographic site i.e. in the oxygen replete layers. The relatively higher

content of ferromagnetic interactions in the octahedral observed in our $SrFe_{0.25}Co_{0.75}O_{2.63}$ further supports the higher frustration at the in-plane interface between the magnetic stacking layers. Thus at the sub-layers scale, the iron and cobalt distribution gives rise to a natural multilayers stacking with dominant nearest neighbor magnetic parallel interactions within the oxygen replete layers and dominant nearest neighbor magnetic anti-parallel interactions within the subsequent oxygen deficient sub-layers. From macroscopic measurements, a ferromagnetic ordered state is found to coexist at low temperatures with a G-type AFM short range ordering. It results in a glassy magnetic state at longer range scale at $T_g = 102.2 \pm 0.15$ K that can be reduced in size when the application of magnetic fields induces a percolation of the FM domains. Such macroscopic phase's separation was previously proposed in $Bi_{0.67}Ca_{0.33}MnO_3$ perovskite manganites [30].

In conclusion, supported by the structural and chemical framework showing subsequent layers along the c axis and following the $Sr_4(Fe_{0.56}^{3+}Co_{1.44}^{3+})^{8h}(Fe_{0.44}^{4+}Co_{0.54}^{4+}Co_{1.02}^{3+})^{8f}O_{10.52}$ paramagnetic cation ordering, complex magnetic properties are reported. The ferromagnetic super-exchange interactions that preferentially takes place on the octahedron 8f sub-layer, give raise to ferromagnetic cluster growth when temperature decreases and/or applied magnetic field increases embedded in a spin cluster glass state below 102.2K. It results in a vertical hysteretic shift on the Field Cooled magnetization isotherm at the ferromagnetic clusters / spin cluster glass matrix interface that becomes giant when percolation of the ferromagnetic clusters occurs.


## Acknowledgement

Author MC acknowledge Université de Bordeaux1 for his PhD fellowship. This work was supported by the European project "SOPRANO" under Marie Curie actions (Grant No. PITNGA-2008-214040).


## Reference


1 S Giri, M Patra and S Majumdar J. Phys.: Condens. Matter **23,** 073201 (2011)
2 W. H Meiklejohn, & C. P. Bean Phys. Rev. **102**, 1413 (1956)
3 J. S. A. Kouvel J. Phys. Chem. Solids **24** 795 (1963)
4 J. Nogues, I.K. J. Magn. Magn. Mater. **192**, 203 (1999)
5 R. Rana, P. Pandey, R.P. Singh, & D.S. Rana Sci. Rep. **4**, 4138 (2014)
6 G. V. M. Williams, E. K. Hemery, and D. McCann Phys. Rev. B **79**, 024412 (2009)
7 Marik S, Mohanty P, Singh D and Singh R P *J. Phys. D: Appl. Phys.* **51** 065006 (2018)

8 R. Ang, Y. P. Sun, X. Luo, C. Y. Hao, X. B. Zhu, and W. H. Song J. Appl. Phys. **104**, 023914 (2008).
9 J. Geshev. J. Appl. Phys. **105**, 066108 (2009)
10 R. Pradheesh, Harikrishnan S. Nair, V. Sankaranarayanan, and K. Sethupathi Appl. Phys. Lett. **101**, 142401 (2012)
11 R. Pradheesh, Harikrishnan S. Nair, C. M. N. Kumar, J. Lamsal, R. Nirmala, P. N. Santhosh, W. B. Yelon, S. K. Malik, V. Sankaranarayanan, and K. Sethupathi, J. Appl. Phys. **111**, 053905 (2012).
12 C. Yin, Q. Liu, R. Decourt, M. Pollet, E. Gaudin, and O. Toulemonde, J. Solid State Chem. **184**, 3228 (2011).
13 O. Toulemonde, J. Abel, C. Yin, A. Wattiaux and E. Gaudin, Chem. Matter. **24**, 1128-1135 (2012)
14 S. Marik, M. Chennabasappa, J. Fernández - Sanjulián, E. Petit and O. Toulemonde, Inorg. Chem. **55**, 9778 (2016)
15 P. Mohanty, S. Marik, D. Singh and R.P. Singh Appl. Phys. Lett. **111** 022402 (2017)
16 J. Fernández Sanjulián, M. Chennabasappa, S. García-Martín, G. Nénert, A. Wattiaux, E. Gaudin, and O. Toulemonde Dalton Trans, **46**, 1624–1633 (2017)
17 S. Srinath, M. M. Kumar, M. L. Post, and H. Srikanth, Phys. Rev. B **72**, 054425 (2005)
18 J. Du, B. Zhang, R.K. Zheng and X.X. Zhang, Phys. Rev. B **75**, 014415 (2007)
19 D.G. Franco, V.C. Fuertes, M.C. Blanco, M.T. Fernandez-Diaz, R.D. Sanchez, R.E. Carbonio J. Solid State Chem, **194**, 385-391 (2012)
20 J. L. Tholence, Solid State Commun. **35**, 113 (1980).
21L. Néel, *Ann. Geophys*. (C.N.R.S.) **5**, 99 (1949).
22 J. Lago, S. J. Blundell, A. Eguia, M. Jansen, and T. Rojo Phys. Rev. B **86**, 064412 (2012).
23 J. L. Tholence Physica **126B** 157-164 (I984)
24 C. N. Guy, J. L. Tholence, H. Maletta, D. J. Thouless, J. A. Hertz, and S. Kirkpatrick Journal of Applied Physics **50**, 7308 (1979) and J. L. Tholence, F. Holtzberg, T. R. McGuire, S. von Molnar, and R. Tournier Journal of Applied Physics **50**, 7350 (1979)
25 J. Souletie and J. L. Tholence Phys. Rev. B **32**, 516(R) (1985)
26 X. Luo, W. Xing, Z. Li, G. Wu, and X. Chen, Phys. Rev. B **75**, 054413 (2007).
27 Vinod Kumar, Rajesh Kumar, Kiran Singh, S. K. Arora, I. V. Shvets, and Ravi Kumar J. Appl. Phys. 116, 073903 (2014)
28 S. Dhara, R.R. Chowdhury, B. Bandyopadhyay Phys Procedia **54**, 38e44 (2014).
29 J. Geshev J. Magn. Magn. Mater. **320**, 600–602 (2008)
30 G. V. M. Williams, E. K. Hemery, and D. McCann Phys. Rev. B **79**, 024412 (2009)
31 M. Giot, A.Pautrat., G. André, D. Saurel, M. Hervieu, and J. Rodriguez-Carvajal,. Physical Review B **77** 134445 (2008)
32 Ch. Binek Phys. Rev. B. **70**, 014421 (2004).
33 D. Paccard, C. Schlenker, O. Massenet, R. Montmory, and A. Yelon, Phys. Status Solidi **16**, 301 (1966).
34I. S. Jacobs and J. S. Kouvel Phys. Rev. **122**, 412 (1961)
35 L. Ghivelder and F. Parisi Phys. Rev. **B** 71, 184425 ( 2005)
36 M. Chennabasappa, E. Petit, O. Toulemonde Ceramics International **46**, 6067-6072 (2020)
37 S. Kawasaki, M. Takano, and Y. Takeda, J. Solid State Chem., **121**, 174 (1996)